A Nonlinear State Observer with Prescribed Exponentially Decaying Normalized Output Injection for SISO and MIMO Systems

TargetDeLab Technical Paper 07

TargetDeLab Group

2026

Abstract

This study investigates a nonlinear state observer with normalized injection of the measured outputs and a prescribed exponentially decaying modulation signal. The actual estimation error is denoted separately by ε(t)=x(t)-$\hat{x}(t)$. If the denominators remain separated from zero, the injection is bounded, integrable, and tends to zero. Asymptotic convergence of ε(t) can be inferred only when the uncorrected error dynamics possess suitable local/incremental stability; detectability alone is not used as a proof of convergence.

Performance is evaluated through the numerical scenarios, sensitivity analyses, Basin of Attraction studies, and Monte Carlo tests accompanying the work. The results show satisfactory tracking for the nonlinear MIMO model examined and low dispersion of the metrics in the specific noise tests. These observations are stated as empirical results for the model under study rather than as a universal guarantee for every detectable nonlinear system.

The main contribution is therefore the investigation of a simple time-varying normalized-output-injection structure exactly as implemented in software, together with numerical mapping of its operating regions.

1 Introduction to Observability of Nonlinear Systems

Observability in nonlinear dynamical systems is a central foundation for observer design and for timely, reliable state estimation in both SISO and MIMO systems. Unlike linear-system theory, in which observability is formulated globally and algebraically through the observability matrix, in nonlinear systems the property is often local, depends on the operating point and the class of inputs (for example persistent excitation), and requires tools from differential geometry and differential algebra for rigorous formulation and analysis [1], [2], [3]. The classical Hermann-Krener observability rank condition provides a local criterion based on the independence of vectors

generated by Lie derivatives of the output functions along the system vector fields and serves as a basic theoretical diagnostic of observability in nonlinear models [1], [2].

There are two complementary families of approaches: (a) analytical-geometric methods that provide theoretical criteria and observer-construction guidelines, and (b) numerical/probabilistic methods that are practical for real, complex MIMO system models.

The first family includes, in addition to differential geometry and Lie derivatives, differential-algebra techniques used for identifiability through manipulation of input-output relations and derivatives. These approaches are particularly useful when the objective is to isolate unobservable parameters or states [4], [13]. This theoretical approach leads to classifications of systems for which observers can be constructed explicitly, such as systems in observer canonical form, and to results on local uniqueness of the reconstructed initial state.

The second family includes practical numerical tools such as the empirical observability Gramian, which estimates output sensitivity to states through perturb-and-observe simulations and is widely used for nonlinear MIMO systems, sensor design, and model reduction [7]. Probabilistic methods include Gaussian-approximation observers such as the Extended Kalman Filter (EKF) and improvements such as the Unscented Kalman Filter (UKF), which handles nonlinear transformation of state distributions more accurately [9], [8], as well as sequential Monte Carlo methods - particle filters - for strongly nonlinear or non-Gaussian problems where the full estimation distribution must be represented by samples [10].

When fast convergence and satisfactory performance are required without strong probabilistic assumptions, deterministic designs such as high-gain observers, nonlinear Luenberger/Gauthier-type observers, and sliding-mode observers have been developed. High-gain designs offer fast convergence but are sensitive to measurement noise, while sliding-mode observers and higher-order sliding differentiators offer robustness to uncertainty but can introduce chattering and require special treatment [5], [11], [4], [6]. Gauthier-type observers and, more generally, geometrically inspired constructions provide systematic design methods when the system satisfies specific structural properties [5], [6].

In applications with unknown inputs or faults, unknown-input and fault-tolerant observers combine observability techniques with mechanisms for isolating or estimating unknown inputs, whereas set-membership/interval observers provide sets of feasible states under bounded-error assumptions. They can therefore give guarantees when probabilistic error distributions are unknown or unreliable [12], [14]. The choice among these methods depends strongly on the type of nonlinearity, the availability of statistical noise models, and the required speed of convergent estimation.

The distinction between SISO and MIMO systems has practical consequences. In SISO systems many issues are simplified and analytical criteria are more readily applicable, whereas in MIMO systems the complexity of Lie derivatives, sensor-placement selection, and input design become critical factors in obtaining a

sufficient observability region. In practice, combining theoretical criteria such as rank conditions with numerical verification using empirical Gramians and Monte Carlo simulations, together with metrics such as condition numbers of the observability map or eigenvalues of the empirical Gramian, is a common and effective evaluation strategy.

Despite major progress in nonlinear observer design, important limitations remain. High-gain observers can be highly sensitive to measurement noise, while stochastic Kalman-type approaches require accurate knowledge of noise statistics and impose increased computational cost in nonlinear MIMO systems. Sliding-mode observers, meanwhile, introduce nonsmooth behavior that may be undesirable in practical applications.

These limitations motivate observer structures that combine design simplicity, smooth dynamic behavior, and intrinsic noise tolerance without requiring strong assumptions or complex transformations.

This study examines a nonlinear observer with normalized output injection and a prescribed exponentially decaying modulation signal. The structure is implemented without Jacobians and without transformation to observer canonical form. Convergence is not attributed to detectability alone; theoretical asymptotic convergence requires additional stability properties of the error dynamics, while performance for the MIMO model considered is documented primarily numerically.

1.1 State Reconstruction, Indistinguishability, and Observability

An observer estimates an unmeasured state x(t) from the known input u(t), measured output y(t), and a mathematical model. The fundamental question is whether distinct initial states can be distinguished by their output histories under the applied input. Two states are indistinguishable over an interval if they produce identical outputs for the same input. A system is observable on a set when indistinguishable initial states cannot occur within that set [1-3]. This definition is global in spirit; practical nonlinear analysis often uses local or weak observability because the input-output map can change with operating point and trajectory.

For smooth systems, local weak observability can be studied through Lie derivatives of the output. Repeated differentiation of h(x) along the vector fields of the dynamics produces scalar functions whose gradients form the nonlinear observability codistribution. A full-rank observability matrix or codistribution at a point is a standard sufficient condition for local weak observability under the corresponding regularity assumptions [1-3]. Unlike the constant observability matrix of an LTI system, this rank can vary across the nonlinear state space.

1.2 Detectability and Observer Convergence Are Distinct Questions

Observability is a property of the plant-output pair; convergence is a property of a particular observer and its error dynamics. Detectability weakens observability

by permitting unobservable components provided that their autonomous behavior is asymptotically stable. In nonlinear systems several nonequivalent formulations are used, including zero-state detectability and output-to-state stability. These notions are useful for excluding unstable hidden dynamics, but they do not imply that every nonlinear observer structure will converge [3,22].

For an observer $\dot{\hat{x}}$=F_o($\hat{x}$,u,y), the estimation error ε=x-$\hat{x}$ obeys a generally nonlinear, time-varying differential equation. A convergence theorem requires a Lyapunov, contraction, incremental-stability, or comparable argument for this error system. This distinction is particularly important for the prescribed-decay observer studied here because its output-injection term tends to zero. Once the injection has faded, long-term convergence depends on the incremental behavior of the plant-copy dynamics.

1.3 Major Families of Nonlinear Observers

Nonlinear observer design does not have a single universal construction. Extended and unscented Kalman filters approximate stochastic state estimation through local linearization or sigma-point propagation. High-gain observers exploit an observable normal form and strong error feedback to obtain rapid convergence, but large gains can amplify measurement noise and produce peaking [5-6,23]. Sliding-mode observers use discontinuous or higher-order correction to obtain robustness against certain uncertainties, at the cost of nonsmooth behavior. Moving-horizon estimation formulates state estimation as a constrained optimization problem over a finite window and can incorporate state and input constraints, but with a substantially higher computational burden.

Another deterministic route generalizes the Luenberger idea by embedding the nonlinear state into coordinates satisfying suitable partial differential equations. The Kazantzis-Kravaris/Luenberger family constructs an auxiliary stable linear system whose state is related injectively to the nonlinear plant state; observer recovery then requires inversion of that mapping [21]. These approaches demonstrate an important theme: provable nonlinear observers typically exchange generality for structural assumptions, computational effort, or sensitivity to noise.

1.4 Robustness, Noise, and Numerical Validation

Measurement noise enters an observer through its innovation or injection channel. Increasing correction gain can accelerate nominal convergence while simultaneously increasing noise transmission. This trade-off is explicit in high-gain observers and is also present, in different forms, in Kalman, sliding-mode, and optimization-based estimators [23,9]. A credible numerical evaluation should therefore report not only a nominal trajectory but also sensitivity to initial conditions, tuning parameters, denominator or singularity conditions, and stochastic noise realizations.

Monte Carlo analysis provides an empirical distribution of performance metrics over repeated noise realizations. It does not by itself prove stochastic stability, but it

can reveal bias, dispersion, failure probability, and nonmonotonic parameter effects that a single run can conceal. Basin-of-attraction sweeps and empirical observability measures similarly complement analytical results by mapping regions in which the implemented algorithm behaves as intended [7]. The later simulations in this chapter are interpreted in this empirical sense.

2 State-Observer Design Methods for Nonlinear Systems

The main state-observer implementation techniques for nonlinear SISO and MIMO systems are summarized below, with reference to both their theoretical foundations and practical implementations. The classical observability conditions and differential-geometric foundation discussed above provide the framework for assessing the suitability of each method [1], [2], [3].

A widely used family of methods is based on local linearization. The Extended Kalman Filter (EKF) linearizes the model about the current estimate and applies classical Kalman filtering, giving a simple and computationally inexpensive algorithm with well-understood tuning, but it has limitations when nonlinearities are strong or the initial estimate is poor [16], [9]. Sigma-point methods, especially the Unscented Kalman Filter (UKF), improve this idea by propagating selected sigma points through the nonlinear dynamics without requiring Jacobians, providing a better approximation of nonlinear transformations at increased cost in high dimensions [8], [9]. When systems are strongly nonlinear or distributions are non-Gaussian, sequential Monte Carlo methods - particle filters - provide a general explicit approximation of the full state distribution by samples, although the cost can become prohibitive in high dimensions without specialized techniques such as Rao-Blackwellization [10].

An alternative practical method that explicitly handles constraints is Moving Horizon Estimation (MHE), in which the estimate is obtained by periodically solving an optimization problem over a moving time window. MHE can handle input/state constraints and provide robustness, but it requires repeated solution of nonlinear optimization problems in real time and proper management of the arrival cost for stability [17].

For fast convergence without probabilistic assumptions, high-gain observers rapidly reduce the estimation error but are sensitive to measurement noise and often require filtering or regularization in practice [5], [6].

Generalizations of the Luenberger structure to nonlinear settings, such as Gauthier-type observers, provide systematic designs with provable asymptotic convergence when the system satisfies the required structural conditions. They cannot be applied arbitrarily to every model because constructing the required transformations can be complex, particularly for MIMO systems [5], [6].

Sliding-mode observers and higher-order sliding differentiators provide characteristic robustness to uncertainties and fast response, but introduce chattering that must be addressed by boundary layers or higher-order designs [11].

For applications with unknown inputs or fault detection/tolerance, unknown-input and fault-tolerant observers combine observability methods with mechanisms that isolate or estimate unknown inputs, often requiring additional structural assumptions on the uncertainties [12]. When reliable statistical error assumptions are unavailable, set-membership or interval observers provide guaranteed sets of feasible states under bounded-error assumptions, which is particularly useful in safety-critical environments, although the sets can become overly conservative in high dimensions without appropriate reduction [14].

For practical design and evaluation, numerical tools such as the empirical observability Gramian estimate local observability using perturb-and-observe methods and are used for sensor selection, input design, and model reduction in complex MIMO systems, complementing analytical criteria [7]. In addition, when worst-case robustness guarantees are required, related nonlinear H-infinity approaches based on Lyapunov-type criteria provide theoretical robustness at increased analytical and computational complexity [9].

The practical choice of method is determined by factors such as state dimension, strength of nonlinearity, availability of statistical noise models, latency/real-time requirements, and computational constraints. In low dimensions with strong nonlinearities, particle filters or UKF may be preferred. In higher dimensions or with limited resources, EKF or reduced-order approaches are more realistic. For constrained systems requiring guarantees, MHE or set-membership methods are valid choices. In practice, hybrid schemes are often selected, for example EKF with a sliding-mode component or EKF/UKF with periodic MHE correction, and empirical tools such as empirical Gramians and Monte Carlo simulations are used for tuning and validation of operating assumptions.

Implementation details differ between SISO and MIMO cases. SISO problems often permit simpler analytical constructions and easier tuning, whereas in MIMO systems Lie derivatives and independence conditions become multivariable and sensor placement and input design become critical to obtaining an adequate observability region. For each implementation, it is advisable to combine theoretical criteria such as Hermann-Krener and differential-algebra checks with numerical verification using empirical Gramians and Monte Carlo analysis, together with systematic benchmarking on SISO and MIMO examples, so that both theoretical support and practical performance are assessed [1], [2], [3], [4], [7], [8], [9], [10], [11], [12], [14], [17].

Despite the broad range of state-estimation approaches for nonlinear systems, no existing class simultaneously satisfies low computational complexity, strong noise robustness, and direct applicability to general nonlinear MIMO systems without structural transformations.

Stochastic methods provide a strong theoretical foundation but require knowledge or estimation of statistical properties and often substantial computational cost. Deterministic high-gain and sliding-mode approaches, although fast, exhibit noise sensitivity or nonsmooth behavior. Constraint- and optimization-based methods such as MHE are likewise computationally demanding for real-time applications.

These limitations motivate new observer structures that combine design simplicity, smooth dynamics, and intrinsic noise robustness without requiring strong statistical or structural assumptions.

The proposed design is a time-varying normalized-output-injection structure. The observer equation and notation follow the MATLAB implementation: the $e^{-\alpha t}$ term appearing in the code is a prescribed modulation signal, not an estimation error.

- No linearization about an operating point or knowledge of Jacobians is required.
- No transformation to observer canonical form or differential-geometric normalization is required.
- The same algorithmic form can be written for SISO and MIMO systems with different numbers of output terms. Effectiveness and convergence must be checked for the specific system and operating region.
- The method does not rely on stochastic assumptions or knowledge of noise covariance models.
- It does not use large constant gains, thereby avoiding strong amplification of measurement noise.
- It exhibits smooth dynamics without chattering.
- It retains low computational complexity and can be implemented in real time.

A distinctive feature is that the corrective injection is a ratio involving measured and estimated outputs multiplied by a prescribed exponentially decaying signal. The influence of the injection therefore decreases with time. This explains the smooth behavior observed numerically, but it also means that long-term convergence depends on the dynamics of the system itself rather than on a permanent innovation-feedback action.

The simulations and Monte Carlo analysis of the model considered show low dispersion in performance metrics for the tested noise realizations. This is numerical evidence of robustness under the specified simulation conditions and cannot be generalized without additional theoretical analysis.

Accordingly, the proposed approach is characterized in this study as a prescribed-decay normalized-output observer. Its contribution is evaluated in terms of structural simplicity, direct MIMO implementation, and numerical results, without claiming universal convergence for general detectable nonlinear systems.

3 Detectability in Nonlinear Systems

Detectability in nonlinear systems is fundamental to observer design and to assessing whether state behavior can be inferred from system outputs. Unlike the LTI case, where detectability has several equivalent definitions and test criteria such as

PBH, in the nonlinear case the concept is generalized in different ways - zero-state detectability, local detectability, output-to-state stability, and others - depending on whether local/global properties or quantitative guarantees are required [2], [3], [6].

Nonlinear detectability theory links classical ideas from Isidori and Sontag with modern approaches such as Lyapunov/OSS analysis, KKL observers, and empirical Gramians. It remains an active research area focused on systematic, practical criteria for observer design in realistic nonlinear environments [2], [3], [6], [21], [7], [19], [20].

3.1 Basic Definitions

Zero-state detectability (local/global): for the nonlinear system $\dot{x}$=f(x), y=g(x) (or with known input u(t)), the pair (f,g) is called zero-state detectable at the equilibrium x=0 if y(t)$\to 0$ as t->infinity implies x(t)$\to 0$ as t->infinity, locally or globally according to the formulation.

This concept states that convergence of the output to zero forces the state vector to converge to zero and is the most direct generalization of LTI detectability [19], [18].

Output-to-state stability (OSS): a quantitative and stronger property. The system is OSS if there exist functions beta of class KL and gamma of class K such that

$$\|x(t)\| \leq \beta(\|x(0)\|, t) + \gamma\left(\sup_{0\leq s\leq t} \|y(s)\|\right).$$

OSS implies zero-state detectability (if y$\to 0$, then x$\to 0$) and also provides a quantitative measure of the rate/sensitivity of the state with respect to the output, useful in robust-observer analysis and in connection with ISS/IOS theory [20], [19].

Local/uniform detectability: often the property of interest is local detectability about an equilibrium or a trajectory. A common definition is that the system is locally detectable about x* if there exists a neighborhood U such that every solution starting in U satisfies y(t)$\to 0$ => x(t)->x*.

Uniform detectability along reference paths/trajectories is also used, with quantitative requirements of consistent behavior.

3.2 Relation to Observability and Implications

Observability implies detectability. The difference is that detectability requires only that nonzero unobservable components do not produce unstable behavior; that is, the “invisible” state components must be asymptotically stable.

In practice, this means that even if every initial state x(0) cannot be reconstructed, it may still be possible to guarantee e(t)$\to 0$ for a state observer provided the unobservable components do not lead to undesirable instability [2], [3].

3.3 Criteria and Analysis Tools

Linearization test (local): linearize about an equilibrium or trajectory and check whether the linear pair (A=partial f/partial x, C=partial h/partial x) is detectable in the LTI sense. Under standard smoothness/Lipschitz conditions this supports local detectability of the nonlinear system.

This is the most common practical test when local behavior of a nonlinear system is of interest [2], [19].

Lyapunov/OSS-type conditions: find a suitable Lyapunov function V(x) satisfying an inequality of the form

$\dot{V}$ <= -W(x) + alpha(|h(x)|)

where W is positive definite. Such an inequality shows that small h implies small V and hence small x, providing OSS/zero-state detectability. The method is useful for quantitative guarantees and connects to observer-Lyapunov constructions for state-observer design [19], [18].

Empirical observability Gramian (numeric): for complex MIMO systems, the empirical Gramian uses perturb-and-observe simulations to estimate output sensitivity to state variables and helps assess local detectability, sensor design, and model reduction [7].

Indistinguishability/differential-algebra approaches: tests based on indistinguishable initial states and differential-algebra methods using input-output relations can provide rigorous, although often demanding, indications of non-identifiability or detectability for specific models [4].

3.4 Relation of Detectability to State-Observer Design

Detectability provides a necessary framework for reconstructing dynamically critical unobservable components, but by itself it is not a sufficient convergence condition for an arbitrary nonlinear observer. Each observer structure requires its own stability conditions. In the proposed structure, because the output injection decays exponentially, asymptotic convergence additionally requires suitable local or incremental stability of the error dynamics.

If the system is not detectable, for example if unobservable components have non-negative or positive real-part modes, there is no general observer that guarantees e(t)$\rightarrow 0$ for all initial states.

3.5 Important Properties and Remarks

Detectability is a fundamental prerequisite for asymptotic convergence of a state observer in nonlinear systems. Even if a system is not fully observable, estimation-error convergence may be achieved when the unobservable components remain asymptotically stable. In practice, local detectability about an operating point or trajectory of

interest is often sufficient for practical nonlinear-observer design, particularly when combined with local linearization or numerical tools such as empirical observability Gramians. Output-to-State Stability (OSS) further provides a quantitative connection between output convergence and state convergence and is a useful framework for robustness and sensitivity analysis under noise and uncertainty.

3.6 Detectability and Practical Observer Design

In practice, detectability is assessed using tools such as local linearization, rank conditions, or empirical observability Gramians. For the proposed structure, these tools characterize the system rather than automatically proving convergence. The theoretical analysis in Section 4 explicitly separates detectability from the additional stability condition required when the corrective injection tends to zero.

4 State Observer with Prescribed Exponentially Decaying Normalized-Output Injection

Plant-observer topology. The nonlinear plant and observer receive the same known input u(t). Measured outputs y=h(x) are supplied to the normalized-output injection term nu, while the observer propagates $\hat{x}$ using the plant model. Performance is evaluated from the actual estimation error x-$\hat{x}$.

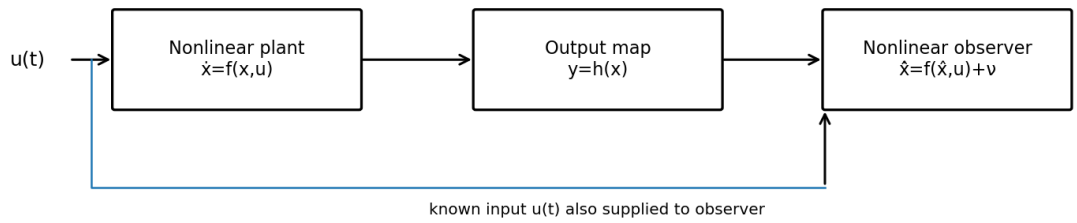


Figure 48. Control topology used in Chapter 7.

Consider the nonlinear system $\dot{x}$=f(x,u), y=g(x,u), with $x \in \mathbb{R}^n$, $u \in \mathbb{R}^m$, and $y \in \mathbb{R}^p$.

$$\dot{x}(t)\text{=f(x(t),u(t))}, \text{ y(t)=g(x(t),u(t))} \tag{1}$$

4.1 Observer Architecture and Computational Algorithm

The implemented observer is organized as a model-copy plus normalized-output-injection architecture. At every integration step the plant and observer receive the same known input $u(t)$. The observer first propagates the model state $\hat{x}$ and computes

the predicted outputs $\hat{y} = g(\hat{x}, u)$. For each state channel i, the prescribed shaping signal $\rho_i(t) = -\alpha_i e^{-\alpha_i t}$ is evaluated. Each measured-output channel k then contributes a normalized correction term whose sign coefficient $A_{ik}(t)$ is selected from the relative signs of y_k and $\hat{y}_k$. The contributions are summed to obtain $\nu_i(t)$ and the observer state derivative is updated as $\dot{\hat{x}}_i = f_i(\hat{x}, u) + \nu_i$.

Algorithmically, one simulation step is therefore: (1) evaluate the plant outputs and observer-predicted outputs; (2) compute the exponentially decaying shaping signals; (3) select the signs of A_{ik}; (4) verify that each denominator $\hat{y}_k - A_{ik}y_k$ remains separated from zero; (5) form and sum the normalized injection terms; (6) integrate the observer model with the known plant input; and (7) compute the actual estimation error $\varepsilon = x - \hat{x}$ only for performance evaluation. The actual state error is not fed directly into the observer law. This separation is central to both the implementation and its interpretation.

4.2 Exact Algorithmic Form of the MATLAB Observer

The observer uses a copy of the model with an additive correction nu(t):

$$\dot{\hat{x}}_i(t) = f_i(\hat{x}(t), u(t)) + \nu_i(t),\ \hat{y}(t) = g(\hat{x}(t), u(t)),\ i = 1, \ldots, n \tag{2}$$

For each state i, a prescribed exponentially decaying modulation signal is defined.:

$$\rho_i(t) = -\alpha_i \exp(-\alpha_i t),\ \alpha_i > 0 \tag{3}$$

The normalized injection is the sum of contributions from the p outputs:

$$\nu_i(t) = \sum_{k=1}^{p} \frac{A_{ik}(t)\,\rho_i(t)\,y_k(t)}{\hat{y}_k(t) - A_{ik}(t)y_k(t)} \tag{4}$$

The sign of $A_{ik}(t)$ changes as in the MATLAB code. For a common magnitude A>0:

$$A_{ik}(t) = +A \text{ if } \operatorname{sign}(y_k(t)) \neq \operatorname{sign}(\hat{y}_k(t));\ A_{ik}(t) = -A \text{ otherwise} \tag{5}$$

The current implementation contains no saturation or threshold function phi(.) in the denominator. The mathematical analysis must therefore make the explicit operating assumption that the denominators do not vanish along the trajectory considered.

$$| \hat{y}_k(t) - A_{ik}(t) y_k(t) | \geq \delta_k > 0, \text{ for all active terms} \tag{6}$$

4.3 Separation of the Shaping Signal from the Actual Estimation Error

The actual observation error is defined independently of $\rho_i(t)$:

$$\varepsilon(t)=x(t)-\hat{x}(t) \tag{7}$$

Using the plant, observer, and injection equations, the actual error dynamics are

$$\dot{\varepsilon}(t)=f(x(t),u(t))-f(\hat{x}(t),u(t))-\nu(t) \tag{8}$$

This distinction is critical: $\rho_i(t)$ is a design signal known in advance and is not computed from $x-\hat{x}$. The observer therefore does not use the unmeasurable state-estimation error in its correction law.

4.4 Boundedness and Asymptotic Behavior of the Injection

If the outputs are bounded, $|y_k(t)| \leq Y_k$, and the separation condition (6) holds, then each component of the output injection satisfies:

$$|\nu_i(t)| \leq \alpha_i e^{-\alpha_i t} \sum_{k=1}^{p} \frac{|A_{ik}|Y_k}{\delta_k} = C_i e^{-\alpha_i t} \tag{9}$$

Hence $\nu_i(t)$ is bounded, absolutely integrable, and tends to zero. The observer is therefore a model with a transient, fading output injection. This property explains why, after the transient stage, the observer approaches the behavior of a free copy of the model.

4.5 Conditional Convergence of the Actual Error

Detectability of the pair (f,g) alone is insufficient to prove $\varepsilon(t) \to 0$ for this particular fading injection. A sufficient local condition is incremental/one-sided exponential stability of the uncorrected dynamics in the operating region Ω:

$$\varepsilon^{T}[f(x,u)-f(\hat{x},u)] \leq -m||\varepsilon||^2,\ m>0,\ x,\hat{x} \in \Omega \tag{10}$$

With $V = \frac{1}{2}\|\varepsilon\|_2^2$ and using (10), one obtains:

$$\dot{V} \leq -m\|\varepsilon\|_2^2 + \|\varepsilon\|_2 C e^{-\alpha_{\min} t} \tag{11}$$

Young's inequality then gives an exponentially decaying forcing term in $\dot{V}$ and, as long as the trajectory remains in Ω and the denominators remain nonzero, the actual error is bounded and converges to zero. Without (11), this work does not claim a global convergence theorem; performance is evaluated numerically.

4.6 Characterization of the Structure

The structure is a nonlinear, time-varying, normalized-output-injection observer. It is not a classical Luenberger, high-gain, or sliding-mode observer. It does not use

covariance propagation and does not require Jacobians. The main tuning parameters are the rate α and magnitude A, while safe operation requires monitoring the denominators $\hat{y}_k$-A_{ik} y_k. The parameter $\alpha > 0$ sets the time scale of the prescribed shaping signal: larger α produces a larger initial magnitude $|\rho_i(0)| = \alpha$ but faster exponential decay, concentrating correction action near the initial transient; smaller α gives weaker but longer-lasting injection. The magnitude $A > 0$ scales the normalized output contribution and also enters its denominator. Increasing A can strengthen the correction but can simultaneously move $\hat{y}_k - A_{ik}y_k$ closer to zero, increasing sensitivity and numerical risk. Consequently α and A must be tuned jointly: α controls when the injection acts, whereas A controls how strongly measured-output mismatch influences the state-copy dynamics.

All observer-performance metrics are computed from the actual state-estimation error $\varepsilon_i(t) = x_i(t) - \hat{x}_i(t)$; their definitions are consolidated in the Mathematical Nomenclature.

5 Simulation of the State Observer for Nonlinear Systems

MATLAB was used for simulation of the nonlinear models in this study. The simulations determine the operation of the state observer for nonlinear MIMO systems. A sampling period dt=0.0001 s (sampling frequency 10 kHz) was used.

The following scenarios are simulated, with their characteristics summarized in the table:

Table 28. Characteristics of the Simulation Scenarios.

Scenario ID	Scenario Characteristics
1	State observer for a nonlinear MIMO system with a four-dimensional state vector, one input, and three outputs
2	Sensitivity analysis of observer parameters α and A for Scenario 1
3	Scenario 1 under the influence of noise

5.1 Scenario 1

Scenario definition. The four-state, one-input, three-output nonlinear MIMO plant and the implemented observer are simulated with Δt=0.0001 s for 100 s. Observer parameters are $\alpha = 0.875$ and $A = 0.5$, and successful tracking means $|x_i - \hat{x}_i| < 0.001$. The known plant input is a step activated at t=50 s; the same input is supplied to the observer.

This scenario simulates the state observer for a nonlinear MIMO system described by the following equations:

$$\frac{dx_1}{dt} = -x_1 + x_2, \quad \frac{dx_2}{dt} = -x_1^2, \quad \frac{dx_3}{dt} = -x_3 - x_2 x_4, \quad \frac{dx_4}{dt} = -x_4 + u \tag{12}$$

$$y_1 = x_1^2 + x_2, \quad y_2 = x_1 x_2, \quad y_3 = -x_1^2 + x_2 x_3$$

with initial conditions $x_1(0) = -1$ and $x_2(0) = x_3(0) = x_4(0) = 1$

5.2 Analysis of Scenario 1 Based on the Observer Implemented in MATLAB

In Scenario 1, the observer uses $\alpha = 0.875$ and $A = 0.5$. For each state, the prescribed shaping signal ρ_i(t)=-0.875 exp(-0.875t) is generated. The three measured outputs enter each component ν_i through three normalized terms.

The actual error used for thresholds, tracking plots, IAE, and the quadratic integral is computed separately from the difference between true and estimated states.

For the model considered, the theoretical requirement that can be checked directly from the observer is that the denominators $\hat{y}_k$-A_{ik} y_k do not approach zero. The local convergence observed in simulation is a combined result of the transient output injection and the local dynamics of the specific model. It is no longer attributed to a general detectability theorem.

5.3 Asymptotic Interpretation and Numerical Region of Attraction

Because ρ_i(t)$\rightarrow 0$, ν_i(t)$\rightarrow 0$ when the denominators remain separated from zero. The error system is therefore asymptotically autonomous, with limiting dynamics $\dot{\varepsilon}$=f(x,u)-f($\hat{x}$,u). This fact alone does not imply that ε=0 is the unique invariant set. Almost-global convergence is not claimed because it does not follow from the MATLAB algorithm without an additional proof of incremental stability.

For this reason, the Basin of Attraction in the next section is explicitly characterized as a numerical/empirical BOA for the selected 2D slices, the specified simulation horizon, and the criterion $|x_i - \hat{x}_i|$<10^{-3}. It is not a global analytical basin.

5.4 Simulation

The parameters used for simulation of the state-observer model are summarized in the table:

Table 29. Observer Parameters.

Parameters	α	**A**
Values	0.875	0.5

The scenario duration is 100 s. The error threshold selected for accurate tracking of the state vector is 0.001. The nonlinear system is excited by a step input, shown in the following figure.

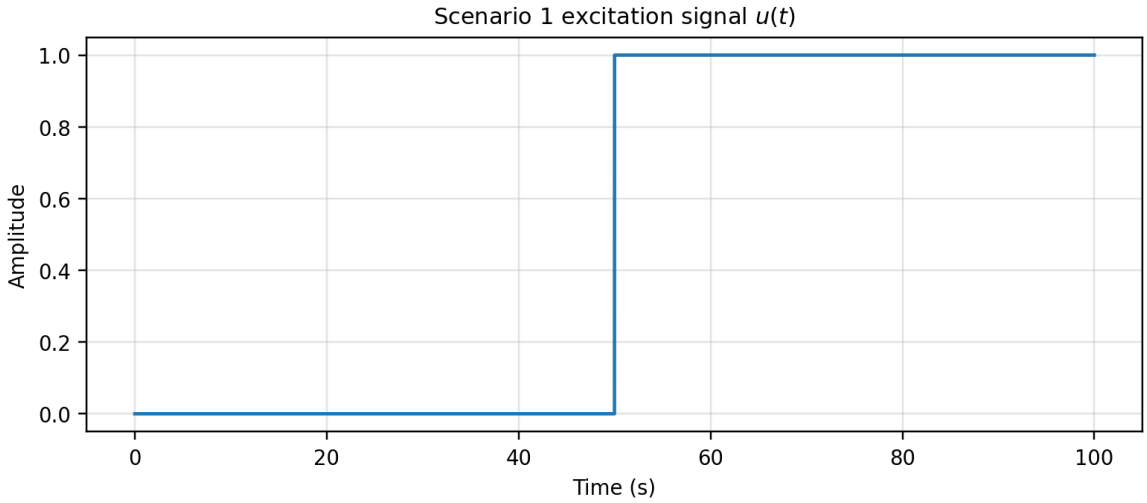


Figure 52. Regenerated system excitation signal in Scenario 1.

The simulation results are shown in the following plots.

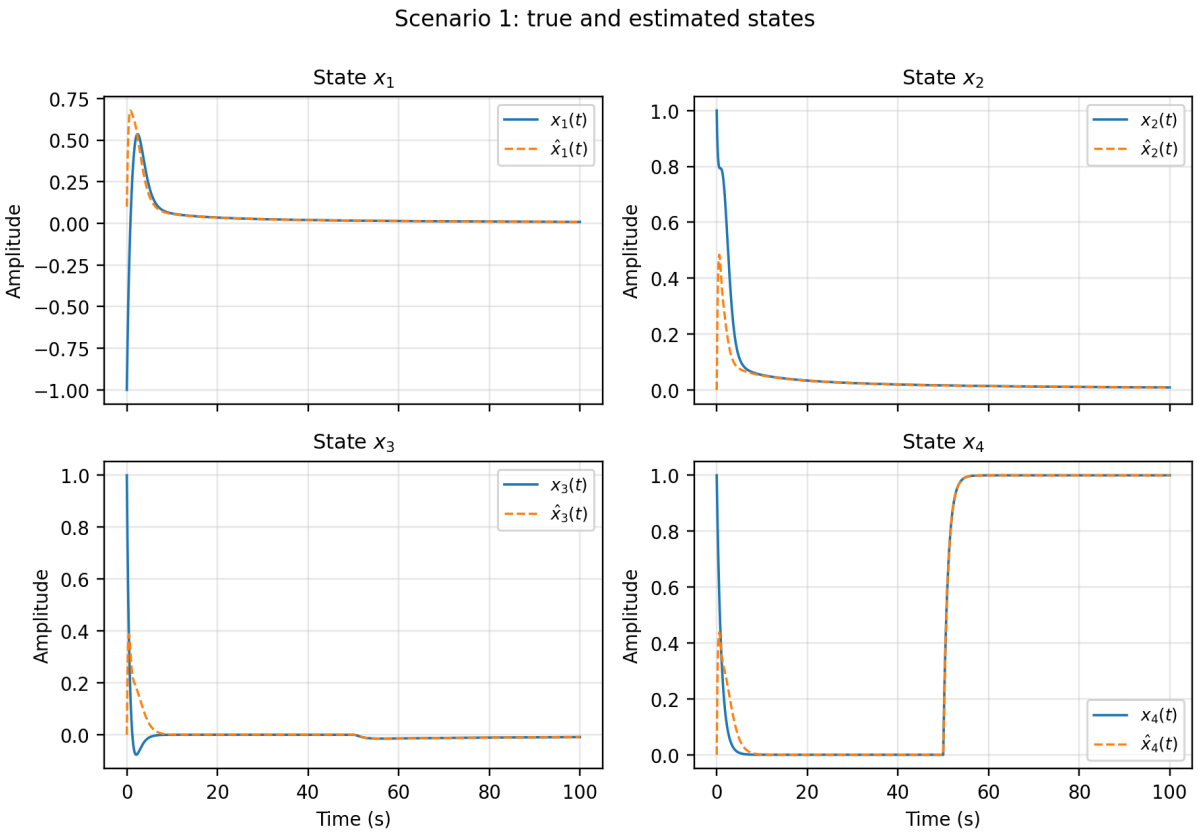


Figure 53. Regenerated true and estimated system states in Scenario 1, arranged as a common 2×2 panel for direct visual comparison.

The results show that the state observer satisfactorily tracks the system state vector. Although the system excitation u(t) is a step activated at t=50 s, it does not impair state tracking because the observer has already converged and its error has become very small.

The following plot shows $e_{\mathrm{IAE}}(t)$ and $e_{\mathrm{ISE}}(t)$ over the simulation interval.

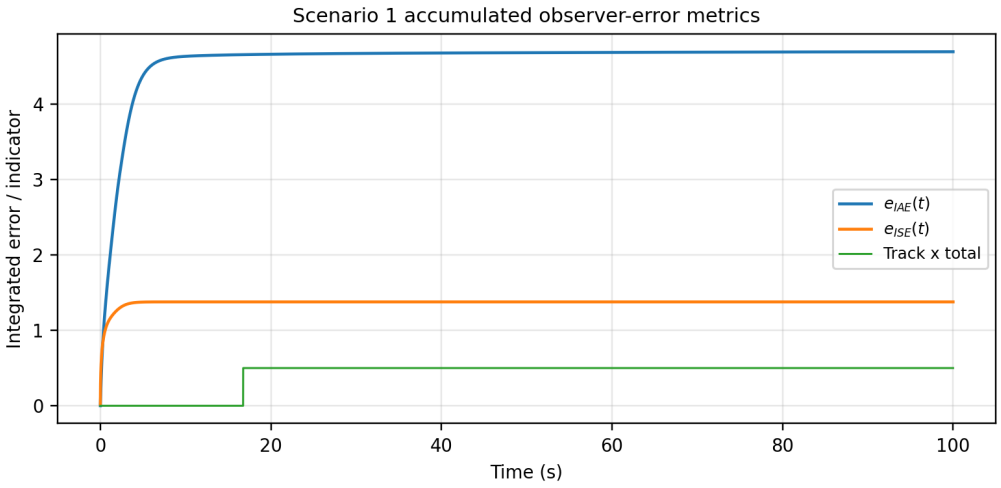


Figure 54. Regenerated accumulated observer-error metrics $e_{\mathrm{IAE}}(t)$ and $e_{\mathrm{ISE}}(t)$, together with the complete-state tracking indicator for Scenario 1.

The $e_{\mathrm{IAE}}(t)$ and $e_{\mathrm{ISE}}(t)$ curves settle to approximately constant steady values after about 18 s, indicating that the state observer has established the tracking levels of the nonlinear-system state variables (Track x Total waveform).

Detailed results for successful state tracking, defined by error below the specified threshold and expressed as a percentage of total simulation time, are summarized in the following table:

Table 30. Scenario 1 Simulation Results.

Quantity	**Value**
x_1(%)	83.266
X_2(%)	84.348
X_3(%)	90.319
x_4(%)	90.089
X_vector(%)	83.255

The results show that the slowest observer convergence mainly concerns state variable x1, which also determines successful tracking of the full nonlinear-system state vector. A state variable is considered converged when the absolute distance |true value - estimated value| is below the threshold 0.001.

5.5 Numerical Computation of the Observer Basin of Attraction

We depict the set of initial errors for which the convergence criterion is satisfied. This defines the numerical Basin of Attraction (BOA) of the observer for the tested setup.

Because the error vector e is four-dimensional, it cannot be displayed directly in a three-dimensional plot for all four variables. We therefore use 2D slices of the error space and select three slices of the form:

- Slice #1: $e_1(0)$–$e_2(0)$, with $e_3(0) = e_4(0) = 0$.
- Slice #2: $e_1(0)$–$e_3(0)$, with $e_2(0) = e_4(0) = 0$.
- Slice #3: $e_2(0)$–$e_4(0)$, with $e_1(0) = e_3(0) = 0$.

The convergence metric is e(T)<ε with T=10 s and ε=`obs_x_thsd`=10^{-3}. The results for the three slices are then presented graphically. The plots use green for convergence regions and red for divergence regions.

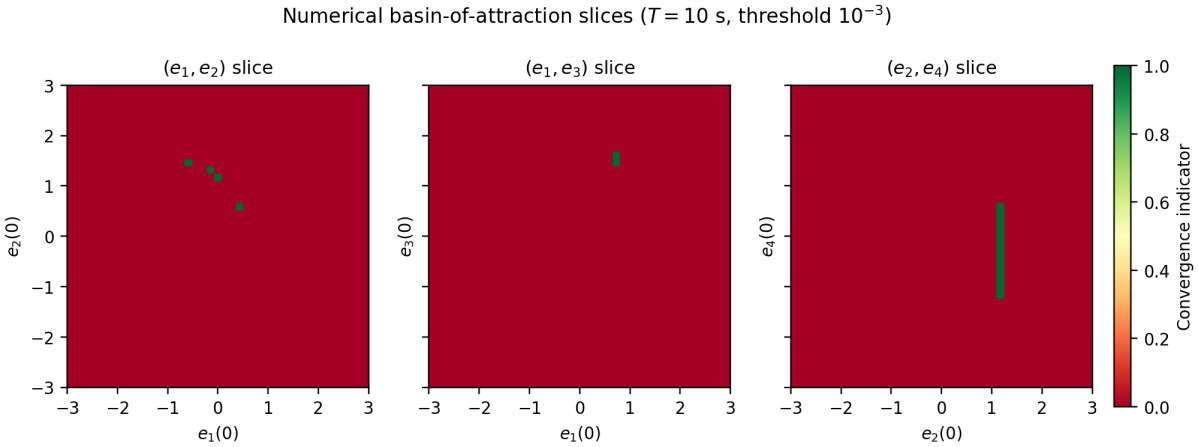


Figure 55. Regenerated numerical Basin of Attraction (BOA) for the three selected two-dimensional slices of the initial estimation-error space.

The regenerated numerical study shows that convergence under the strict terminal criterion is not obtained over the whole tested square. Instead, each two-dimensional slice contains a comparatively narrow region of initial estimation errors that converges to the specified threshold within the 10 s horizon. This result is more conservative than the earlier raster visualization and reinforces the interpretation of Figure 55 as an empirical, finite-horizon region of attraction rather than evidence of global or almost-global convergence.

5.6 Scenario 2

Scenario definition. The plant, initial setup, 100 s horizon, and 0.001 tracking threshold of Scenario 1 are retained while observer parameters α and A are swept. A coarse grid uses $\Delta\alpha$=ΔA=0.1; a finer grid then uses 0.025 increments around the best region. Tracking percentage over the full interval is the sensitivity metric.

This simulation scenario examines sensitivity of the Scenario 1 observer model to parameters α and A. Simulations were first performed over the selected parameter intervals with steps $\Delta\alpha$=0.05 and ΔA=0.05. The coarse sensitivity results are shown in Figure 56.

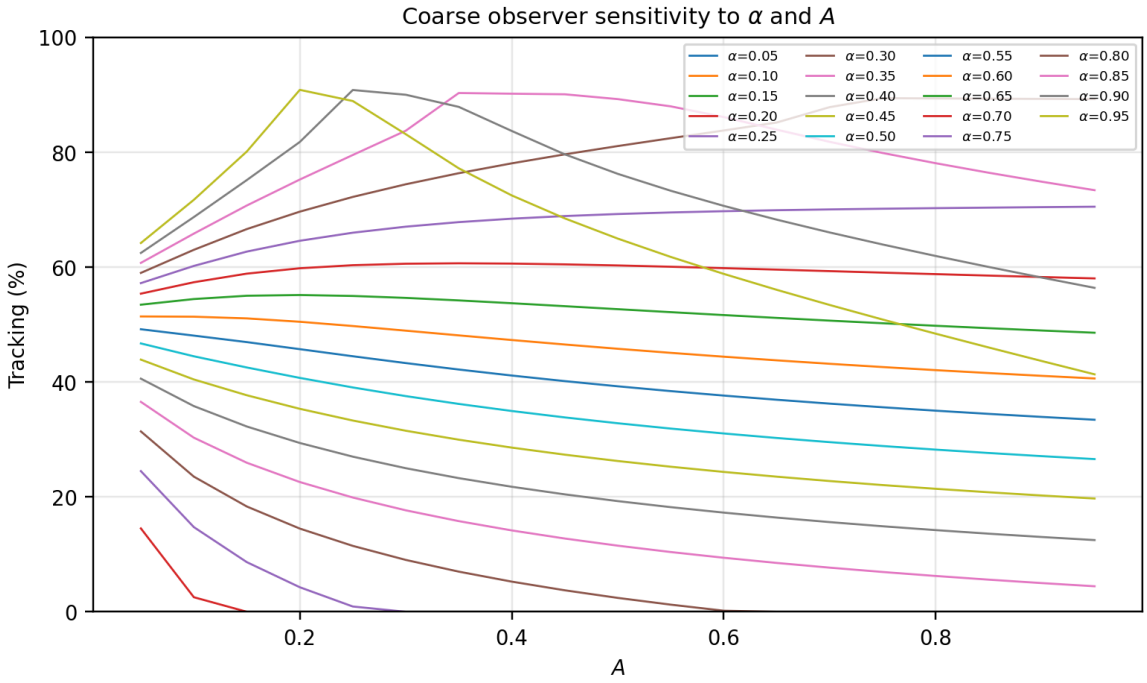


Figure 56. Regenerated coarse observer sensitivity with respect to parameters α and A for Scenario 1.

The results show the effect of observer parameters α and A on the ability to track the system states. Successful tracking is reported as the percentage of the total 100 s simulation interval for which all state variables have settled to errors below the threshold 0.001 (`obs_x_thsd`=0.001). The coarse sweep reveals strong dependence on both parameters and several high-performance combinations rather than a flat tuning region. A finer search is then performed with steps $\Delta\alpha$=0.025 and ΔA=0.025 in the selected high-performance neighborhood. The refined sensitivity map is shown in Figure 57.

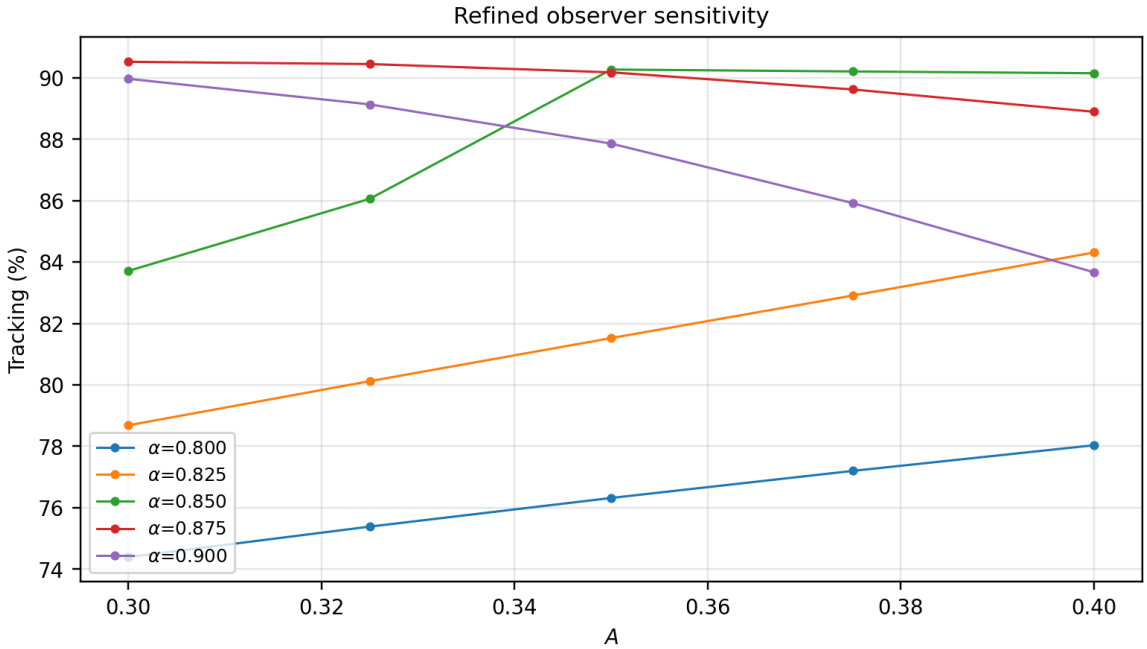


Figure 57. Regenerated refined observer sensitivity with respect to parameters α and A for Scenario 1.

The choices $\alpha = 0.875$ and $A = 0.30$ give the highest tracking percentage (90.5238%).

The two-stage parameter sweep shows that observer tuning is not arbitrary. The broad high-performance region in the coarse map indicates that satisfactory behavior is not confined to a single isolated parameter pair, while the refined search identifies a local best value for the chosen tracking-percentage criterion. This result should be interpreted as empirical tuning for the stated plant, initial conditions, threshold, and 100 s interval; it does not imply that the same α and A are optimal for other nonlinear systems.

5.7 Scenario 3

Scenario definition. Scenario 1 is repeated with additive white Gaussian measurement noise applied to the three plant outputs; the illustrated case uses -20 dB noise. All other plant, observer, input-step, sampling, duration, and threshold settings are retained. The subsequent Monte Carlo study repeats this noisy-output configuration 100 times for each tested noise level.

This scenario simulates the state observer for the nonlinear MIMO system of Scenario 1 in the presence of additive white Gaussian noise of specified power at the system outputs, representing measurement-device noise. All other simulation conditions are retained from Scenario 1.

5.8 Simulation

The output signals of the nonlinear MIMO system under additive white Gaussian noise at -20 dB are shown in the following plot:

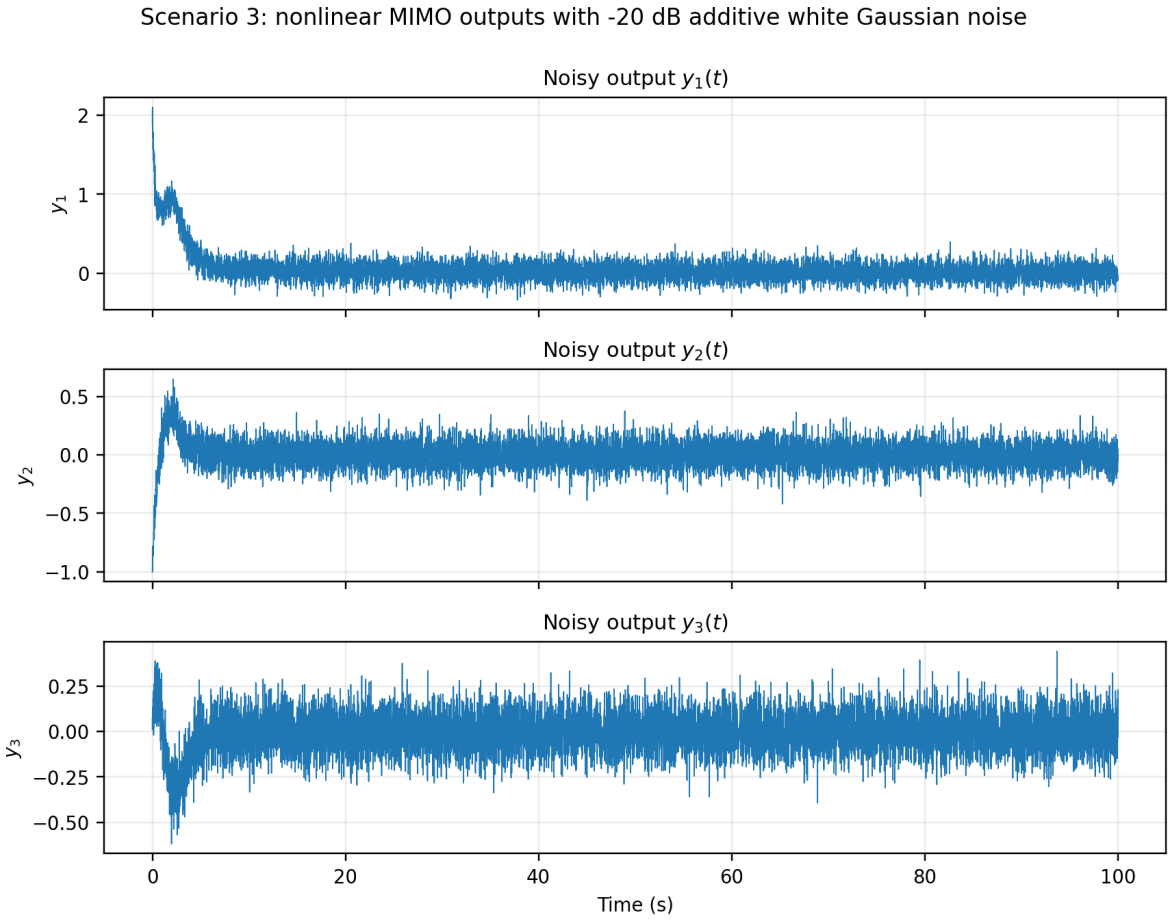


Figure 58. Regenerated nonlinear MIMO output signals under -20 dB additive white Gaussian measurement noise.

The noise is very pronounced at the outputs of the nonlinear MIMO system. The simulation results are shown in the following plots.

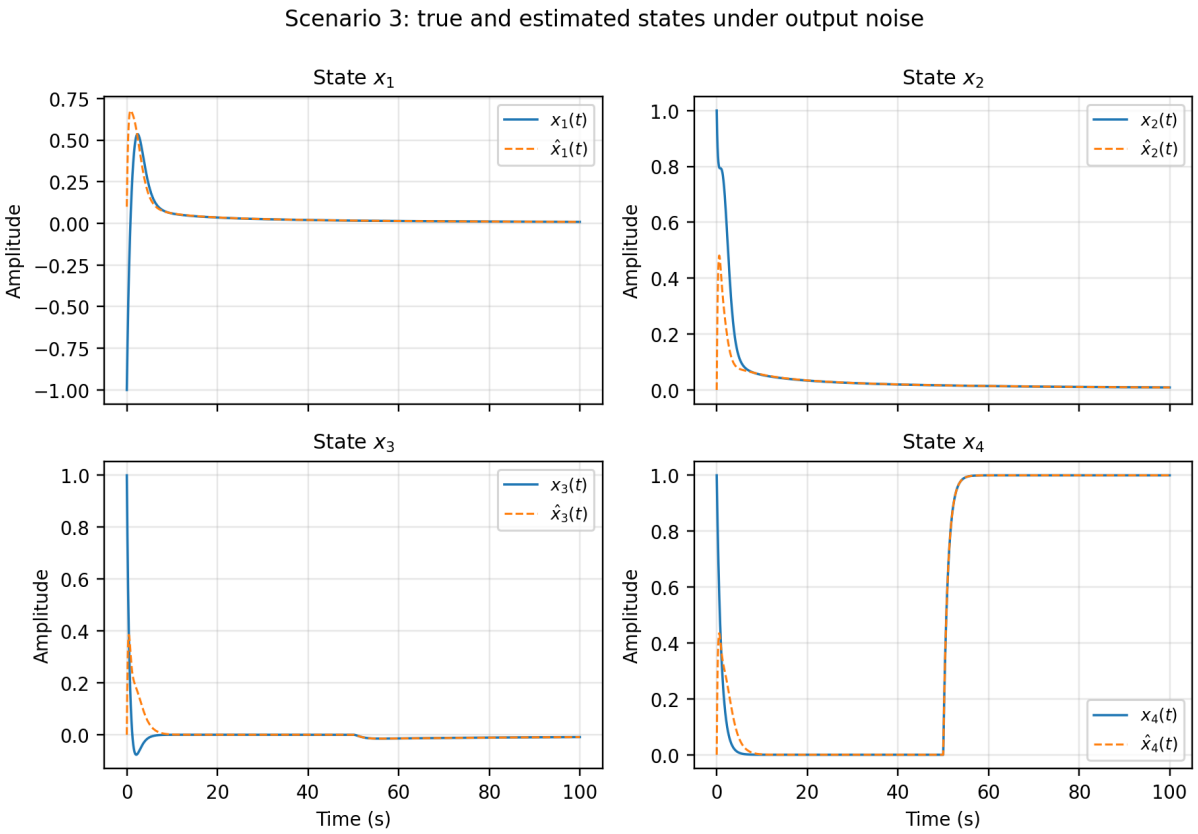


Figure 59. Regenerated true and estimated system states in Scenario 3 under output noise, arranged as a common 2×2 panel.

The simulation plots show that the state observer satisfactorily tracks the system state vector despite the noise acting on the outputs. The estimated-state waveforms remain smooth despite the output noise. Although the excitation u(t) is a step activated at t=50 s, it does not impair state tracking because the observer has already converged.

The important feature is that convergence established before the input step is not lost when the excitation changes at t=50 s. The estimated trajectories remain close to the true states even though the measured outputs are visibly noisy, indicating that the implemented injection does not simply reproduce the measurement fluctuations in the state estimates. This observation is qualitative evidence of useful noise tolerance for the tested case and is quantified further by the accumulated-error and tracking-percentage metrics.

The following plot shows $e_{\mathrm{IAE}}(t)$ and $e_{\mathrm{ISE}}(t)$ over the simulation interval.

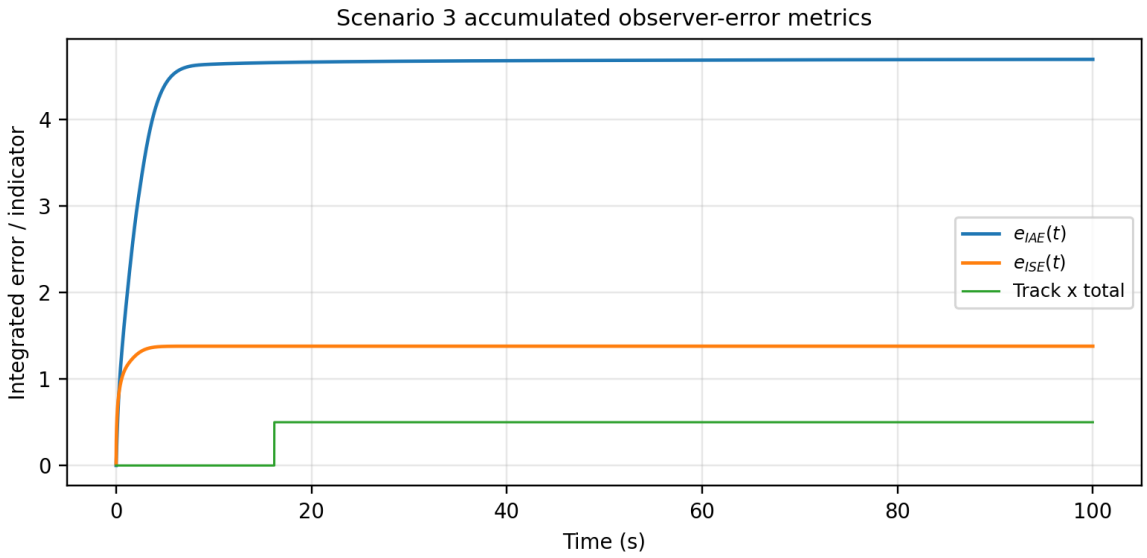


Figure 60. Regenerated accumulated observer-error metrics $e_{\mathrm{IAE}}(t)$ and $e_{\mathrm{ISE}}(t)$, together with the complete-state tracking indicator for Scenario 3.

The $e_{\mathrm{IAE}}(t)$ and $e_{\mathrm{ISE}}(t)$ curves settle to approximately constant steady values after about 18 s, indicating that the state observer has restored the tracking levels of the nonlinear-system state variables (Track x Total).

Detailed tracking results, expressed as a percentage of total simulation time, are summarized in the following table:

Table 31. Scenario 3 Simulation Results.

Quantity	**Value**
x_1(%)	85.156
X_2(%)	86.154
X_3(%)	89.877
x_4(%)	89.642
X_vector(%)	83.700

The results show that the slowest observer convergence again mainly concerns state variable x1, which determines tracking of the complete nonlinear-system state vector. A state variable is considered converged when the absolute distance between the true and estimated values is below the 0.001 threshold. State-vector observation remains satisfactory despite the noise acting on the system outputs.

Because complete-vector tracking requires every state to satisfy the 0.001 error threshold, the slowest state becomes the limiting factor in the reported Track x Total percentage. This explains why strong tracking of x2 and x3 cannot compensate for delayed convergence of x1 in the aggregate metric. The table should therefore be read both state by state and as a vector criterion; the latter is intentionally conservative.

5.9 Monte Carlo Analysis of Observer Performance under Output Noise in the Nonlinear MIMO System

Monte Carlo simulations were then performed under the same conditions as Scenario 3, using 100 repetitions for different output-noise levels. The results are summarized in the table:

Table 32. Monte Carlo Simulation Results.

Noise levels (dB)	Mean IAE	Std IAE	Mean ISE	Std ISE	Mean Track Util	Std Track Util
-40	4.697	0.00042862	1.3772	4.2576e-05	83.268	0.045884
-30	4.6626	0.0010872	1.3771	0.00011113	88.365	0.043491
-20	4.6929	0.0013916	1.3785	0.00033345	83.755	0.15633
-10	4.9732	0.0026893	1.4118	0.00064625	73.144	0.14496
0	5.6271	0.0082415	1.5335	0.0011215	88.075	0.18977

Mean denotes the ensemble mean and Std the standard deviation over the 100 simulation runs.

5.10 Behavior of IAE and ISE

The IAE and ISE indices show a clear tendency to increase as the noise level increases, which is expected because noise introduces additional fluctuations in the estimation error. The best performance in IAE and ISE occurs for noise levels between -40 dB and -30 dB, where the minimum overall deviation is obtained.

The relatively low dispersion (standard deviation) of the metrics at all noise levels indicates that observer behavior is consistent across different stochastic noise realizations. This suggests low sensitivity to the random realization of the noise and provides empirical evidence of stochastic robustness under the tested conditions.

The Monte Carlo dispersion is particularly important because it distinguishes a repeatable trend from an accidental result of one noise realization. Small standard deviations indicate that the reported mean behavior is representative of the tested ensemble. At the same time, the nonmonotonic Tracking Utilization trend shows that different metrics can respond differently to the same noise level; increased accumulated error can coexist with a larger fraction of time inside a threshold. For this reason, no single observer metric should be used in isolation.

5.11 Behavior of the Tracking Utilization Index

Unlike IAE and ISE, the Tracking Utilization index exhibits nonmonotonic behavior with respect to noise level:

- At low noise levels (-40 dB to -30 dB), performance improves and reaches a maximum near -30 dB.

- At intermediate noise levels (-20 dB to -10 dB), performance degrades significantly, reaching a minimum at -10 dB.
- At high noise level (0 dB), the index improves again and approaches the performance observed at low noise levels.

This behavior indicates a nonlinear interaction between the noise and the observer dynamics.

5.12 Interpretation of the Nonmonotonic Behavior

The observed nonmonotonic behavior can be interpreted as follows:

- Low noise levels (-40 to -30 dB): the noise is sufficiently small not to degrade estimation and may at the same time provide mild excitation that increases the information available to the observer from the outputs.
- Intermediate noise levels (-20 to -10 dB): the noise becomes strong enough to disturb the estimation process without providing a beneficial excitation effect. This region forms a degradation zone in which the influence of noise is predominantly adverse.
- High noise level (0 dB): the noise acts as strong stochastic excitation and, in the observed simulations, reduces the time for which the error remains in regions of large deviation. The Tracking Utilization index therefore increases even though the total error also increases. This is an empirical observation and is not, by itself, evidence of a general stochastic-resonance mechanism.

5.13 General Characterization with Respect to Noise

Based on the above numerical results, the proposed observer can be characterized for the tested model as follows:

- It is robust to the tested noise realizations in the empirical sense that satisfactory performance is retained even at high noise level (0 dB), without observed instability or severe degradation.
- It exhibits low stochastic sensitivity, as indicated by the small dispersion of the metrics over all Monte Carlo repetitions.
- Its performance depends nonlinearly on noise level, with distinct low-, intermediate-, and high-noise operating regions in which the influence of noise differs qualitatively.
- The simulations indicate that strong stochastic excitation can alter the fraction of time for which the error remains within acceptable limits; this observation is reported as a model-specific numerical result.

5.14 Concluding Observation

The results show that the effect of noise on the proposed observer is not simply destabilizing but exhibits more complex behavior that depends on noise level. This makes the observer structure interesting for applications with substantial stochastic measurement fluctuations, while the observed behavior still requires system-specific validation.

6 Conclusions

This study examined a nonlinear observer with prescribed exponentially decaying normalized-output injection. The mathematical description is consistent with the MATLAB implementation: variables e1,...,en in the code are prescribed shaping signals ρ_i(t)=-α_i exp(-α_i t), not the actual state errors. The actual estimation error is defined independently as ε=x-$\hat{x}$.

The output injection is a sum of terms $A_{ik}\ \rho_i\ y_k$/($\hat{y}_k$-$A_{ik}\ y_k$), with the sign of A_{ik} changed according to the comparison of sign(y_k) and sign($\hat{y}_k$). With bounded outputs and denominators separated from zero, the injection is bounded, integrable, and tends to zero. Asymptotic convergence of the actual error additionally requires suitable local/incremental stability of the limiting error dynamics. Detectability remains an important property of the system but is no longer presented as a sufficient proof of convergence for this specific observer structure.

The numerical tests of the MIMO system considered show satisfactory tracking, broad success regions in the tested 2D slices of initial errors, clear dependence on parameters α and A, and low Monte Carlo dispersion over the noise levels studied. These results constitute empirical evidence for the specific model and settings.

Overall, the simulation campaign provides three complementary kinds of evidence: trajectory plots demonstrate qualitative state reconstruction, basin/sensitivity sweeps map where the chosen implementation performs satisfactorily, and Monte Carlo trials test repeatability under stochastic output perturbations. These results strengthen confidence in the observer for the specific model without replacing the missing general convergence proof. The most defensible conclusion is therefore empirical and conditional: the observer performs well over the tested regions when the denominator terms remain well behaved and the limiting error dynamics are favorable.

The nonmonotonic behavior of Tracking Utilization versus noise remains an interesting numerical finding, but it is not interpreted as a general stochastic-resonance or self-regularization property without additional stochastic analysis. Likewise, claims of global or almost-global convergence are restricted to what the simulations support.

Future work should focus on: (i) analytical conditions guaranteeing denominator separation, (ii) ISS/delta-ISS or contraction conditions for the error dynamics, (iii) a regularized denominator formulation for guaranteed numerical well-posedness, and

(iv) benchmarking against EKF/UKF, high-gain, and other nonlinear observers on the same models and noise levels.

Relationship to the Complete Book

This paper is a self-contained study extracted and reformatted from the corresponding research chapter of *Nonlinear Control: From Model to Evidence*. The complete book provides the unified progression across all seven studies, cross-study synthesis, extended methodological context, and the MATLAB/Octave and Python software-companion architecture used for replication and further experimentation.

6.1 References

[1] R. Hermann and A. J. Krener, “Nonlinear controllability and observability,” IEEE Transactions on Automatic Control, vol. AC-22, no. 5, pp. 728–740, 1977.

[2] A. Isidori, Nonlinear Control Systems, 3rd ed., Springer, 1995.

[3] E. D. Sontag, Mathematical Control Theory: Deterministic Finite Dimensional Systems, 2nd ed., Springer, 1998.

[4] M. Fliess, J. Levine, P. Martin and P. Rouchon, “Flatness and defect of non-linear systems: introductory theory and examples,” International Journal of Control, vol. 61, no. 6, pp. 1327-1361, 1995. DOI: 10.1080/00207179508921959.

[5] J.-P. Gauthier, H. Hammouri and S. Othman, “A simple observer for nonlinear systems: applications to bioreactors,” IEEE Transactions on Automatic Control, vol. 37, no. 6, pp. 875-880, 1992. DOI: 10.1109/9.256352.

[6] G. Besançon, Nonlinear Observers and Applications, Springer, 2007.

[7] S. Lall, J. E. Marsden and S. Glavaski, “A subspace approach to balanced truncation for model reduction of nonlinear control systems,” International Journal of Robust and Nonlinear Control, vol. 12, no. 6, pp. 519-535, 2002. DOI: 10.1002/rnc.657.

[8] S. J. Julier and J. K. Uhlmann, “A new extension of the Kalman filter to nonlinear systems,” Proceedings of AeroSense, 1997.

[9] D. Simon, Optimal State Estimation: Kalman, H Infinity, and Nonlinear Approaches, Wiley, 2006.

[10] A. Doucet, N. de Freitas and N. Gordon (eds.), Sequential Monte Carlo Methods in Practice, Springer, 2001.

[11] V. I. Utkin, Sliding Modes in Control and Optimization, Springer, 1992.

[12] J. Chen and R. J. Patton, Robust Model-Based Fault Diagnosis for Dynamic Systems, Kluwer Academic Publishers, 1999.

[13] E. Walter and L. Pronzato, Identification of Parametric Models from Experimental Data, Springer, 1997.

[14] M. Milanese and A. Vicino, “Optimal estimation theory for dynamic systems with set membership uncertainty: an overview,” Automatica, vol. 27, no. 6, pp. 997-1009, 1991. DOI: 10.1016/0005-1098(91)90134-N.

[15] R. E. Kalman, “A new approach to linear filtering and prediction problems,” Transactions of the ASME—Journal of Basic Engineering (Series D), 1960.

[16] A. Gelb (Ed.), Applied Optimal Estimation, MIT Press, 1974.

[17] J. B. Rawlings and D. Q. Mayne, Model Predictive Control: Theory and Design, Nob Hill Publishing, 2009.

[18] H. K. Khalil, Nonlinear Systems, 3rd ed., Prentice Hall, 2002.

[19] D. Angeli, “A Lyapunov approach to incremental stability properties,” IEEE Transactions on Automatic Control, vol. 47, no. 3, pp. 410–421, 2002.

[20] Z.-P. Jiang, A. R. Teel and L. Praly, “Small-gain theorem for ISS systems and applications,” Mathematics of Control, Signals and Systems, vol. 7, no. 2, pp. 95-120, 1994. DOI: 10.1007/BF01211469.

[21] N. Kazantzis and C. Kravaris, “Nonlinear observer design using Lyapunov’s auxiliary theorem,” Systems & Control Letters, vol. 34, no. 5, pp. 241-247, 1998. DOI: 10.1016/S0167-6911(98)00017-6.

[22] E. D. Sontag and Y. Wang, “Output-to-state stability and detectability of nonlinear systems,” Systems & Control Letters, vol. 29, no. 5, pp. 279-290, 1997.

[23] H. K. Khalil and L. Praly, “High-gain observers in nonlinear feedback control,” International Journal of Robust and Nonlinear Control, vol. 24, no. 6, pp. 993-1015, 2014. DOI: 10.1002/rnc.3051.